Magnetic Resonance in Medicine 55:279–286 (2006)

Investigating Brain Metabolism at High Fields using Localized ^{13}C NMR Spectroscopy without ^{1}H Decoupling

Dinesh Kumar Deelchand,* Kâmil Uğurbil, and Pierre-Gilles Henry

Most in vivo ^{13}C NMR spectroscopy studies in the brain have been performed using ^{1}H decoupling during acquisition. Decoupling imposes significant constraints on the experimental setup (particularly for human studies at high magnetic field) in order to stay within safety limits for power deposition. We show here that incorporation of the ^{13}C label from ^{13}C-labeled glucose into brain amino acids can be monitored accurately using localized ^{13}C NMR spectroscopy *without* the application of ^{1}H decoupling. Using LCModel quantification with prior knowledge of one-bond and multiple-bond J_{CH} coupling constants, the uncertainty on metabolites concentrations was only 35% to 91% higher (depending on the carbon resonance of interest) in undecoupled spectra compared to decoupled spectra in the rat brain at 9.4 Tesla. Although less sensitive, ^{13}C NMR without decoupling dramatically reduces experimental constraints on coil setup and pulse sequence design required to keep power deposition within safety guidelines. This opens the prospect of safely measuring ^{13}C NMR spectra in humans at varied brain locations (not only the occipital lobe) and at very high magnetic fields above 4 Tesla. Magn Reson Med 55:279–286, 2006.

Key words: 13C NMR spectroscopy; LCModel; decoupling; specific absorption rate; long-range couplings

^{13}C NMR spectroscopy with the use of ^{13}C-enriched substrates is a unique tool to study metabolic pathways for energy and neurotransmitter metabolism non-invasively in the brain (1–3). Whether direct or indirect detection were utilized, most in vivo ^{13}C NMR spectroscopy studies have used decoupling during acquisition in order to improve signal-to-noise ratio (S/N) and reduce spectral overlap.

In general, decoupling imposes severe experimental constraints, particularly in human studies at high magnetic fields, due to the necessity to keep the specific absorption rate (SAR) within the safety guidelines issued by the U.S. Food and Drug Administration (FDA) (4) or International Electrotechnical Commission (IEC) (5). These limits become even more constraining at high magnetic field as SAR increases with static magnetic field (B_0) (6). In addition, the distribution of B_1 radiofrequency field becomes highly inhomogeneous and sample dependent at high field, rendering very difficult the accurate prediction of local high-SAR values (the so-called hot spots) in the brain (7,8). These factors have so far limited the development of ^{13}C NMR in humans to fields no higher than 4 Tesla (9,10). Only one preliminary study (11) (published in abstract form) has reported the necessity to increase the repetition time at 7 Tesla in order to ensure that SAR remained within the FDA guidelines.

Another consequence of decoupling is that most studies in the human brain have been performed in the occipital lobe. This may be attributed in part to constraints imposed by decoupling on RF coil design (use of surface coils, minimization of coil coupling, and electrical isolation between ^{13}C and ^{1}H tune-matched circuits). In addition, potential eye damage for measurements in brain areas close to the eyes, such as the frontal lobe, when using decoupling has also been a concern. In many cases, therefore, decoupling represents a major obstacle when implementing ^{13}C NMR spectroscopy methodology in human studies. One recent study proposed a method for indirect detection of ^{13}C label in the monkey brain using ^{1}H PRESS sequence without ^{13}C editing or decoupling (12). Although some studies have measured ^{13}C glycogen signal without ^{1}H decoupling (13), quantification of ^{13}C-labeled glutamate and glutamine in the brain using ^{13}C NMR spectroscopy without ^{1}H decoupling has not been reported.

To alleviate the constraints imposed on ^{13}C NMR spectroscopy experiments by the use of ^{1}H decoupling, we evaluated the feasibility of using ^{13}C NMR spectroscopy *without* the application of proton-decoupling to measure the incorporation of ^{13}C label from ^{13}C-labeled glucose into brain metabolites. Interleaved undecoupled and ^{1}H-decoupled ^{13}C spectra were measured in the rat brain at 9.4 Tesla during infusion of [1,6-$^{13}C_2$] glucose or [1-^{13}C] glucose. Spectra were quantified using LCModel (14) with prior knowledge of one-bond and long-range J_{CH} coupling constants measured on high-resolution NMR spectra of metabolites in solution. The accuracy and precision of quantification of both decoupled and undecoupled spectra was evaluated using Monte-Carlo simulations.

METHODS AND MATERIALS

Measurement of J_{CH} Coupling Constants

500 mM solutions of glutamate, glutamine, and aspartate (Sigma Chemical Co., St Louis, MO, USA) were prepared in 10% D_2O and 90% H_2O. The pH of each solution was corrected to be in the range 7.10–7.20, and ^{13}C NMR spectra were recorded at 37°C on a 14.1 Tesla UNITY INOVA spectrometer (Varian, Palo Alto, CA, USA) using a pulse-acquire sequence with NOE and using either no ^{1}H decoupling or selective (continuous) ^{1}H decoupling as de-

Center for Magnetic Resonance Research, Department of Radiology, University of Minnesota Medical School, Minneapolis, MN 55455, USA.

Grant Sponsor: NIH; Grant Number: P41RR00789. Grant Number: R01NS38672. Grant Sponsor: the MIND institute. Grant Sponsor: the Keck Foundation. The high-resolution NMR facility at the University of Minnesota is supported with funds from the NSF (BIR-961477), the University of Minnesota Medical School, and the Minnesota Medical Foundation.

*Correspondence to: Dinesh Deelchand, Center for Magnetic Resonance Research, 2021 6th Street, SE, Minneapolis, MN 55455, USA. E-mail: dinesh@cmrr.umn.edu

Received 30 June 2005; revised 31 August 2005; accepted 22 September 2005.

DOI 10.1002/mrm.20756

Published online 2 December 2005 in Wiley InterScience (www.interscience.wiley.com).

scribed below (repetition time of 15 s, 58 K data points, acquisition time of 1 s or 2 s). All FIDs were averaged to 128 scans or until sufficient S/N was achieved. Exponential decay function (LB) of 0.2 Hz was applied before Fourier transformation and line fittings were performed using the Varian built-in software.

J-couplings values from one-bond and long-range CH in glutamate and aspartate were measured on selective proton-decoupled and undecoupled NMR spectra after deconvolution. Since peaks overlapped at some carbon positions in the undecoupled spectra (due to different chemical shift of protons (15) attached to the same carbon), selective proton-decoupling (at low power) was applied to measure these long-range couplings. The one-bond couplings, on the other hand, were measured from the undecoupled data.

A complication to measure long-range J_{CH} coupling constants for glutamine was the presence of protons in the amide group (-$CONH_2$) at the 5th carbon position (denoted as C5), which resulted in additional splitting of the C4 carbon resonance. Although the two amide protons H_Z and H_E are not equivalent (resonating at 6.82 and 7.53, respectively), H_E exchanges rapidly with water (16) and therefore had no apparent J-coupling with neighboring carbons (as observed from selective proton-decoupled ^{13}C spectra). The three bond coupling between C4 and H_Z was resolved by applying selective (continuous) decoupling simultaneously to the H2 and H3 protons of glutamine at 3.75 ppm and 2.14 ppm, respectively, using an amplitude modulated radiofrequency waveform.

Animal Preparation and Glucose Infusion

All studies were approved by the Institutional Animal Care and Use Committee at the University of Minnesota. Following an overnight fast, rats ($n = 4$, weight 278 ± 4 g; means ± SD) were induced with a mixture of 30% oxygen, 70% nitrous oxide, and 5% isoflurane, intubated, and maintained anesthetized with 1.8% isoflurane. Two femoral arteries were cannulated for measuring blood gases and glucose levels and for monitoring arterial blood pressure. A femoral vein was cannulated for i.v. infusion of glucose. In addition, an intraperitoneal (i.p.) line was inserted for administration of morphine sulfate and pancuronium. After surgery, the isoflurane was replaced by a bolus injection of morphine sulfate (50 mg/kg) and pancuronium (1.0 mg/kg) before continuous infusion (35.2 mg/kg/hr) of a mixture of morphine sulfate and pancuronium in a molar ratio of 3:1.

The animal was placed in a cradle and the head secured with a bite-bar and ear rods. The RF coil was placed on top of the head. The body temperature was monitored throughout the study with a rectal thermo sensor and maintained at 37°C using a hot water circulation tube. Animals were infused with labeled glucose (either [1-^{13}C] or [1,6-$^{13}C_2$]) based on a protocol used previously (17,18). In short, during the first 5 min, a 99%-enriched glucose bolus was administrated, followed by a continuous infusion of 70%-enriched glucose thereafter. Two of the rats were infused with [1,6-$^{13}C_2$] glucose, while the remaining two were infused with [1-^{13}C] glucose.

In Vivo ^{13}C NMR Spectroscopy

In vivo ^{13}C NMR spectra from rat brain were obtained as previously described elsewhere (17,18). Briefly, a 9.4 Tesla horizontal bore magnet was used with a half-volume quadrature transmit and receive radiofrequency probe consisting of a ^{13}C surface coil and quadrature ^{1}H coils. The pulse sequence consisted of a 3D ^{1}H-localization using a combination of outer-volume-suppression (OVS) and ISIS followed by polarization transfer via a semi-adiabatic DEPT sequence. A volume-of-interest (VOI) of 400 μL (9 × 5× 9 mm^3) was positioned in the rat brain with the aid of transverse and sagittal RARE images. Shimming on the VOI was performed using FAST(EST)MAP (19), resulting in a water linewidth between 18 to 28 Hz. A repetition time (TR) of 2.5 s was used and 8 K of data points (N) was collected in blocks of 128 scans, giving a spectral time resolution of 5.33 min. In all experiments, proton decoupling (WALTZ-16) was switched on and off in an interleaved fashion after every block of 5.33 min.

Quantitation of In Vivo Spectra

All in vivo spectra were analyzed using LCModel (14) version 2.3 (Stephen Provencher Inc., Oakville, ON, Canada). The basis sets for LCModel were generated by simulating spectra for every observable isotopomer in Matlab (The MathWorks Inc., Natick, MA, USA) using the proton-carbon coupling constants (J_{CH}) measured in this study and published values of ^{13}C chemical shifts and homonuclear ^{13}C-^{13}C couplings (J_{CC}) from Henry et al. (18). No baseline correction, zero-filling, or apodization functions were applied to the in vivo data prior to LCModel analysis. Relative concentrations obtained from LCModel were converted to absolute concentrations by assuming a glutamate pool size of 10.0 μmol/g in the brain and using the fractional enrichment of each metabolite (calculated from isotopomer in the in vivo data). A correction factor was applied to account for transfer efficiency resulting from DEPT.

Monte-Carlo Simulations

The accuracy and precision of LCModel quantitation was assessed by Monte-Carlo simulation. For each Monte-Carlo simulation, glutamate and glutamine spectra at 9.4 Tesla were simulated (either with or without ^{1}H decoupling). The relative percentage of each isotopomer in simulated spectra was chosen to be similar to that found in the rat brain at isotopic steady-state after infusion of [1,6-$^{13}C_2$] labeled glucose (18) or [1-^{13}C] glucose to mimic in vivo conditions. Gaussian noise with a chosen root-mean-square (RMS) value was added to simulated spectra, and LCModel quantitation was performed 200 times with a different noise (but identical rms noise level). S/N was defined as the ratio of the peak height of Glu-C4 singlet to twice the rms noise level. The Monte-Carlo procedure was then repeated for different rms noise levels.

RESULTS

^{13}C Spectral Pattern of Amino Acids without ^{1}H Decoupling

Undecoupled ^{13}C NMR spectra exhibit extensive splitting due to one-bond and long-range couplings compared to

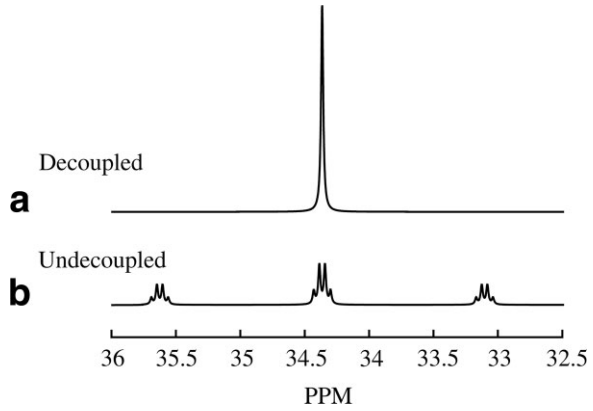

FIG. 1. Comparison between proton-decoupled (**a**) and undecoupled (**b**) ^{13}C spectra of [4-^{13}C] glutamate. Data were simulated at 9.4 Tesla with N = 10 K, spectral width SW = 18000 Hz, and LB = 2 Hz.

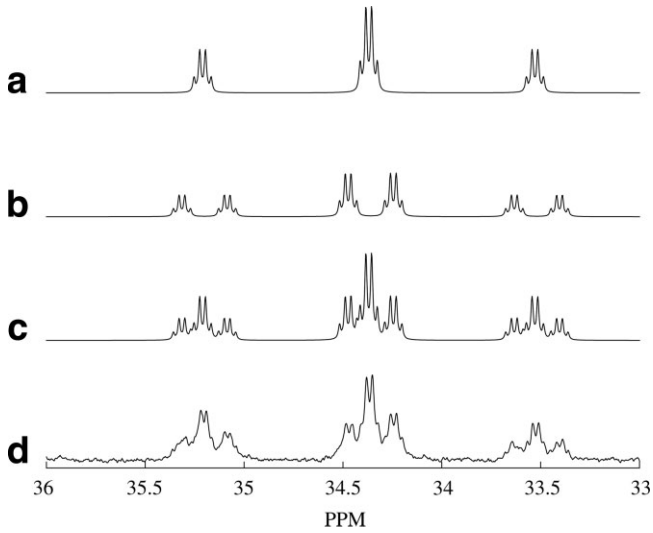

FIG. 2. Simulated undecoupled ^{13}C NMR spectrum of C4 peak resonance of glutamate at 14.1 Tesla (N = 10 K, SW = 18000 Hz, LB = 2 Hz) due to J_{CH} couplings alone (**a**) whereby each line is split into a doublet due to J_{CC} coupling of 34.5 Hz (**b**) and the resultant spectrum due to these couplings (**c**). ^{13}C NMR of a brain extract (**d**) (infused with [1,6-$^{13}C_2$] glucose) acquired without ^{1}H decoupling on a 14.1 Tesla INOVA spectrometer (N = 180 K, SW = 30000 Hz, TR = 15s, 1400 scans, NOE enhancement, and LB = 1 Hz).

decoupled spectra (Fig. 1). The simulated spectrum of [4-^{13}C] glutamate with ^{1}H decoupling shows a single resonance line at 34.4 ppm (Fig. 1a). In contrast, undecoupled spectra of [4-^{13}C] glutamate show 12 distinct resonances (Fig. 1b). The two directly attached protons at the C4 carbon position result in a triplet separated by $^{1}J_{CH}$ = 126.79 Hz (Table 1). Moreover, long-range couplings from protons at C2 and C3 carbon are large enough to result in noticeable splitting of the C4 carbon resonance ($^{2}J_{CH}$ = 4.52 Hz and $^{3}J_{CH}$ = 4.31 Hz). Because $^{2}J_{CH}$ and $^{3}J_{CH}$ have nearly similar values, the resulting spectrum appears as a triplet of quadruplets (Fig. 1b).

Spectra of glutamate from brain extracts after infusion of [1,6-$^{13}C_2$] glucose exhibit an even more complex spectral pattern due to the presence of multiply labeled isotopomers (Fig. 2). When glutamate is labeled at the C4 position but not at the C3 position, the resulting C4 spectrum appears as a triplet of quadruplets, referred as Glu-C4S (Fig. 2a). In contrast, when glutamate is labeled at both C4 and C3 positions (noted Glu-C4D43 following the nomenclature used by Jeffrey et al. (20)), resonances are further split due to carbon-carbon coupling J_{CC} = 34.5Hz (Fig. 2b). The resultant ^{13}C NMR spectrum is a combination of spectra from Glu-C4S and Glu-C4D43 (Fig. 2c). The simulated spectrum is in agreement with an experimental proton-undecoupled ^{13}C spectrum from a rat brain extract obtained after the animal was infused with [1,6-$^{13}C_2$] glucose for 7 h (18) (Fig. 2d). Therefore, prior knowledge of Glu-

Table 1
Measured J-coupling Values of 3 Metabolites Under Physiological Conditions (37°C, pH of 7.15) Presented as Mean ± Standard Error (SE)

Metabolite	Group	Mean coupling ± SE (Hz)		
		$^{1}J_{CH}$	$^{2}J_{CH}$	$^{3}J_{CH}$
Aspartate				
	^{2}CH	144.40 ± 0.01	3.07 ± 0.03 3.91 ± 0.03	—
	$^{3}CH_2$	129.20 ± 0.11	4.49 ± 0.01	—
Glutamate				
	^{2}CH	145.14 ± 0.08	4.20 ± 0.01	4.07 ± 0.05
	$^{3}CH_2$	130.45 ± 0.04	4.29 ± 0.04	—
	$^{4}CH_2$	126.79 ± 0.03	4.52 ± 0.02	4.31 ± 0.03
Glutamine				
	^{2}CH	145.46 ± 0.04	4.21 ± 0.04	3.78 ± 0.03
	$^{3}CH_2$	131.36 ± 0.03	4.64 ± 0.03[a] 4.82 ± 0.04[b]	—
	$^{4}CH_2$	128.41 ± 0.04	4.47 ± 0.03	4.47 ± 0.03 6.7[c]

[a]Proton at C2 position.
[b]Proton at C4 position.
[c]Coupling between glutamine-C4 with amide proton H_Z (no SE available).

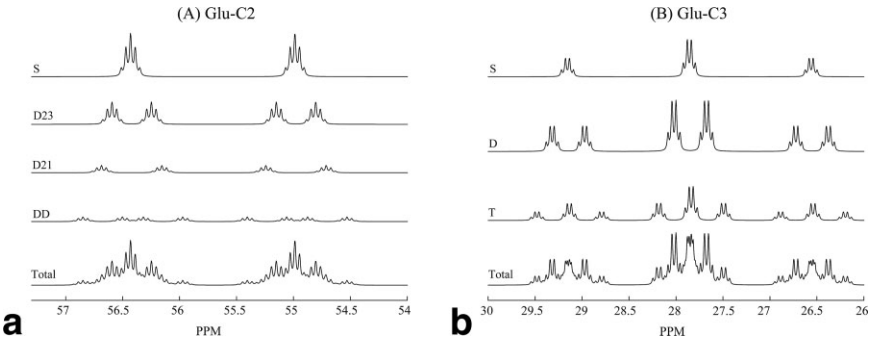

FIG. 3. Simulated undecoupled ^{13}C spectra of (**a**) glutamate C2 (Glu-C2) and (**b**) glutamate C3 (Glu-C3) at 9.4 Tesla obtained after administrating [1,6-$^{13}C_2$] glucose under steady-state condition (N = 10 K, SW = 18000 Hz, LB = 2 Hz). Top spectra show splittings due to J_{CH} couplings only (represented by S). Each resonance is further split due to appropriate ^{13}C-^{13}C couplings. The resultant spectrum in each case is represented at the bottom (total). D: doublet; T: triplet; DD: doublet of doublets.

C4S and Glu-C4D43 (Figs. 2a and 2b) is expected to represent sufficient prior knowledge for LCModel to reproduce spectral features of in vivo undecoupled ^{13}C spectra under these infusion conditions.

In a similar way, the C2 carbon resonance of glutamate labeled at the C2 position but not C1 and C3 (Glu-C2S) appears as a doublet of quintuplets (Fig. 3a) due to the combined effect from one-bond coupling from the proton directly attached to C2 ($^1J_{CH}$ = 145.14 Hz) and the long-range coupling from protons attached to C3 and C2 positions ($^2J_{CH}$ = 4.20 Hz and $^3J_{CH}$ = 4.07 Hz). The C2 resonance of glutamate in the brain after infusion of ^{13}C-labeled glucose is further split due to the effect of ^{13}C-^{13}C coupling and can be accounted for as a superposition of spectra of Glu-C2S, Glu-C2D21, Glu-C2D23, and Glu-C2DD (Fig. 3a).

The C3 carbon resonance of glutamate labeled at C3 position but not C2 and C4 shows 12 resonance lines (Glu-C3S; Fig. 3b), similar to that of C4 resonance (Glu-C4S), due to directly attached protons at C3 ($^1J_{CH}$ = 130.45 Hz) and the two-bond couplings from C2 and C4 positions, which were identical ($^2J_{CH}$ = 4.29 Hz). Furthermore, due to homonuclear carbon-carbon couplings, as obtained under in vivo condition when administrating labeled glucose, the C3 resonance is split into a doublet (Glu-C3D) and a triplet (Glu-C3T). The combination of these isotopomers (Glu-C3S, Glu-C3D, and Glu-C3T) results in a complex spectrum (Fig. 3b).

In Vivo ^{13}C NMR Spectra of Rat Brain

The undecoupled spectrum acquired in vivo for 3½ hours after the start of [1,6-$^{13}C_2$] glucose infusion in the rat brain has lower sensitivity in comparison to the decoupled case (Fig. 4a). The resonances corresponding to glucose C6, glutamate C4, C3, C2, glutamine C4, C3, C2, and aspartate C2, C3 were clearly resolved in both proton-decoupled and undecoupled spectrum, although the latter case has more peaks overlap primarily due to the one-bond J_{CH} coupling constant. No major overlaps between metabolites were observed in the undecoupled case, with the exception of glutamate and glutamine C4 resonances; in this case, one of the lateral resonances of these carbons coincides with one another, as evidenced by a much higher resonance amplitude in the undecoupled spectrum (Fig. 4a). In addition, low concentration ^{13}C-labeled metabolites, such as γ-aminobutyric acid (GABA) and N-acetyl-aspartate (NAA), were also detected in the decoupled spectrum, while not that apparent in the undecoupled spectrum due to lower peak S/N ratio.

The in vivo ^{13}C time course spectra (Fig. 4b) obtained from a volume of 400 μL was acquired in an interleaved

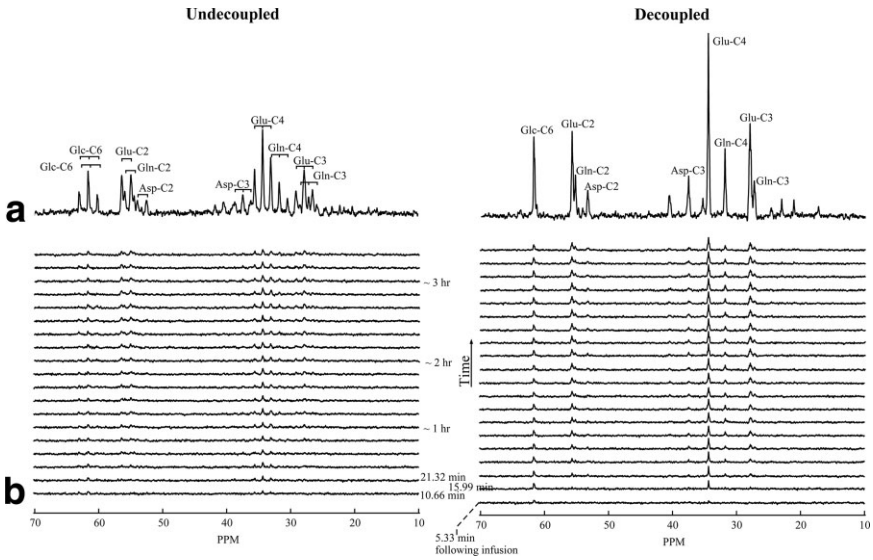

FIG. 4. Localized ^{13}C NMR spectrum of the rat brain in vivo (acquired in alternation) without (left column) and with (right column) WALTZ-16 broadband proton-decoupling during 3½ hours infusion of [1,6-$^{13}C_2$] glucose. (**a**) The summed time course spectra of decoupled and undecoupled data (2560 averages). (**b**) Spectral time series undecoupled and decoupled ^{13}C spectra, with a time difference of 5.33 min between each plot (128 scans each with TR of 2.5 s). All spectra were zero-filled to 128 K and a 5 Hz exponential decay and 1.8 Hz Gaussian functions were applied prior to FT. Glc: glucose; Glu: glutamate; Gln: glutamine; and Asp: aspartate.

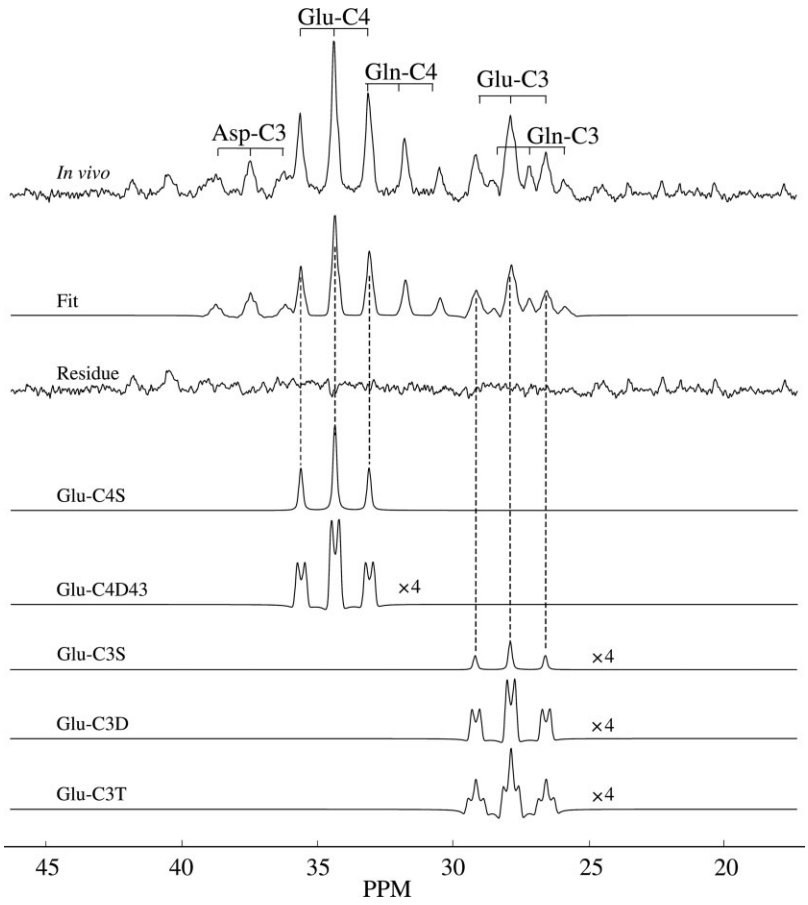

FIG. 5. LCModel fit of an in vivo undecoupled ^{13}C spectrum. From top to bottom: the in vivo spectrum, the best fitted spectrum, the residue left after subtracting the reconstructed spectrum from the original one and the decomposition of the individual isotopomers contributing to glutamate C4 and C3 peaks. All individual isotopomers fit were scaled by a factor of 4, except that of Glu-C4S. Effect due to J_{CC} modulation was clearly visible in the ^{13}C-^{13}C isotopomer fits. Only the spectral region from 20 to 45 ppm was shown here.

fashion with a temporal resolution of 5.33 min (decoupled and undecoupled spectra on the right and left, respectively). The peak signal to noise was lower by about 2.5 in the undecoupled data as observed in the stacked plots.

The residuals, obtained after LCModel analysis of the summed undecoupled in vivo spectrum of Fig. 4a, showed a nearly flat spectrum in the region from 25 to 40 ppm with minimal signals present, indicating an efficient fitting algorithm (Fig. 5). Since low concentration metabolites, such as GABA, NAA, and lactate, were not considered in the basis set, their resonances were still present in the residuals. LCModel analysis also allowed the determination of individual isotopomers contributing to each resonance, such as glutamate C4 and C3, as demonstrated in Fig. 5.

^{13}C Concentration Time Courses

The in vivo time courses of undecoupled (open symbols) data were in excellent agreement with those of proton-decoupled (filled symbols) for both glutamate and glutamine resonances (Fig. 6). Although the SD was increased when no decoupling was applied, the concentration of the individual resonances remained unbiased in either ^{13}C-labeled glucose infusion. Quantification of undecoupled spectra resulted in a coefficient of variation of 35% to 91% higher than that of decoupled spectra.

When the time courses were compared for the two differently labeled glucose used ([1,6-$^{13}C_2$] and [1-^{13}C]), in either the decoupled and undecoupled time series, a higher S/N was in general evident in the case of doubly labeled glucose as the metabolic precursor. The average coefficient of variation was 5.2% and 9.0% at steady-state condition for undecoupled glutamate-C4 when administrating [1,6-$^{13}C_2$] and [1-^{13}C] glucose, respectively.

Simulations

Monte-Carlo simulations showed an increase in the Cramer-Rao bound (CRB) of 52%, 100%, and 73% when determining metabolite concentrations for undecoupled glutamate C2, C3, and C4, respectively, in comparison to decoupled with administration of [1,6-$^{13}C_2$] glucose (Fig. 7). The total concentrations of undecoupled resonances of glutamate C2, C3, and C4 were unbiased at low signal-to-noise ratio (CRB $\leq$ 10%). In the decoupled case, the errors of the estimated concentrations were not significant at low S/N values.

Determination of the individual isotopomers of glutamate-C4 (i.e., Glu-C4S and Glu-C4D43) using undecoupled data indicated that an S/N ratio of at least 2 was required to accurately measure their concentrations (data not shown). Similar results were obtained for C2 and C3 glutamate.

Simulations performed for the case when [1-^{13}C] glucose was infused showed similar loss in CRB when comparing decoupled to undecoupled data (data not shown). However, use of this substrate leads to two-fold decrease in the

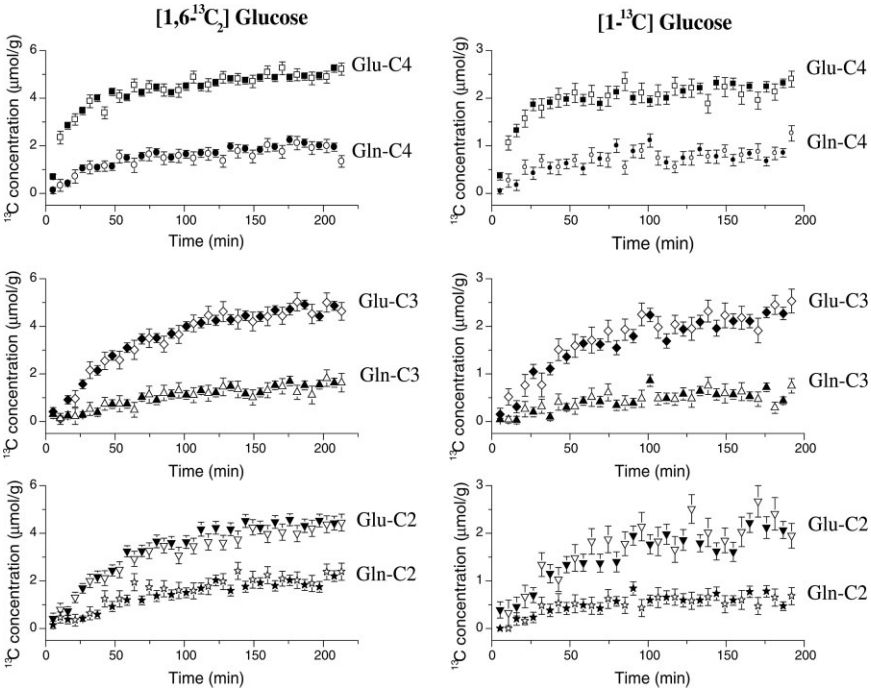

FIG. 6. In vivo time course of incorporation of ^{13}C labels into glutamate (C4, C3, and C2) and glutamine (C4, C3, and C2) in the rat brain after administration of either [1, 6-$^{13}C_2$] glucose (left) or [1-^{13}C] glucose (right). Filled and open symbols represent decoupled and undecoupled data, respectively.

sensitivity due to lower proportion of multiplets due to ^{13}C-^{13}C homonuclear couplings relative to multiplets due to ^{13}C-^{1}H couplings (as found in the in vivo data above).

DISCUSSION

This study demonstrates the feasibility of accurately quantifying undecoupled ^{13}C NMR spectra with LCModel using prior knowledge of chemical shifts and J-coupling values. Although the peak signal-to-noise ratio was decreased by a factor of 2.5 in undecoupled spectra compared to decoupled spectra at 9.4 Tesla, ^{13}C metabolite concentrations remained unbiased and their coefficient of variation was only 35% to 91% higher when quantified from undecoupled spectra, in excellent agreement with Monte-Carlo simulations (52% to 100%). This comes about because of incorporation of prior knowledge into the spectral analysis algorithm about the undecoupled spectral patterns of the resonances due to one-bond and long range couplings. Performing ^{13}C NMR spectroscopy *without* ^{1}H decoupling has the potential to significantly reduce experimental constraints on RF design and power deposition imposed by decoupling.

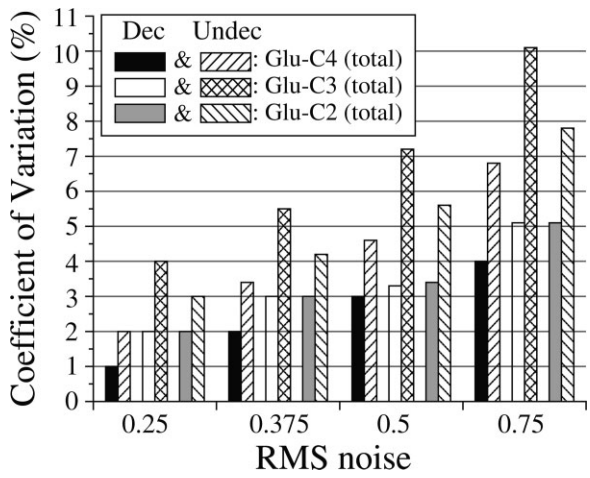

FIG. 7. Effect of different rms noise levels on the coefficient of variation (%) of total isotopomers concentration of C2, C3, and C4 glutamate from Monte-Carlo simulations when administrating [1, 6-$^{13}C_2$] glucose. Both undecoupled (striped bar) and decoupled (filled bar) data are compared, and each bar represents 200 synthetic data sets. Rms noise of 0.5 corresponds to a peak S/N of 3.2 (8.4) for undecoupled (decoupled) NMR.

RF Coil Design

An important issue to consider for a successful ^{13}C NMR spectroscopy experiment when applying ^{1}H decoupling during acquisition is the requirement of excellent electrical isolation (21) between the ^{13}C and ^{1}H RF channels. Experiments with decoupling often require the use of RF filters and careful adjustment of the RF coil setup to avoid injection of unwanted noise into the receiver during decoupling (22,23). Without decoupling, the ^{1}H coil(s) will still be needed for NOE or polarization-transfer in order to enhance ^{13}C signal, but requirements on electrical isolation between the two channels would be much less stringent. The use of RF filters would no longer be necessary, and a more flexible RF coil design could be used. For instance, using a freely movable ^{13}C coil embedded within a ^{1}H volume or arrayed coil will be useful for acquiring localized data in the brain (24) (when using the 3D ^{1}H-localized ^{13}C detection sequence as above). Therefore, data could be collected anywhere from the brain without the risk of damaging low-perfused tissues like the eyes, instead of the routine acquisition from the occipitoparietal lobe as in most cases for ^{13}C spectra in human brains (25–27).

SAR Limitation

Using either direct or indirect ^{13}C detection techniques, signal decoupling is generally applied during acquisition. Even so, RF power deposition (mainly due to decoupling) within a specific tissue is a critical issue to consider for human studies in both cases, as recommended by international guidelines (4,5) the maximum SAR allowed over the head is 3.0 W/kg averaged for 10 min exposure to RF fields.

RF decoupling is restricted for human applications at high magnetic fields (28) mainly due to limits on local tissue heating since power deposition increases with static magnetic field strength (29). Unfortunately, determination of local SAR level (7,8) is very difficult to achieve due to non-homogeneity of B_1 field. Although recent studies have used FDTD simulations in a model of the human head to predict local SAR in the head (30), local SAR may vary from one subject to the next due to the natural anatomic heterogeneity across subjects. There has only been one attempt to do in vivo ^{13}C NMR spectroscopy in humans at 7 Tesla using adiabatic proton-decoupling with surface coils, by Gruetter et al. (11) in 2001, whereby the major problem was SAR limitation. No other study to investigate human brain metabolism has so far been reported at these high fields. In order to maintain SAR within the FDA guidelines, a longer repetition time (5 s) was required in this study, performed in the occipital lobe, leading to approximately a factor loss of $\sqrt{2}$ in sensitivity compared to a TR of 2.5 s. Proton decoupling in deeper structure would require higher power, thus even longer repetition time, so that ^{13}C NMR without ^{1}H decoupling would become advantageous. The technique of acquiring undecoupled ^{13}C NMR spectra is also a safer approach as one does not need to work at the limit of allowed SAR. Furthermore, some of the sensitivity lost by not applying decoupling may be recovered by reducing the repetition time. Alternatively, in order to retain high S/N in the spectrum and also reduce SAR, decoupled spectra can be acquired in between every n^{th} ($n > 1$) undecoupled spectra, as demonstrated by the interleaved fashion utilized in this article. The decoupled spectra can thus be used as a reference when fitting undecoupled data by applying appropriate constraints in the analysis.

Undecoupled ^{13}C NMR Spectroscopy in Humans

High field systems result in higher spectral and spatial resolution (31). For example, at 4 Tesla the C2 resonances of glutamate and glutamine are not well resolved (separation of 0.5 ppm in between). However, at 9.4 Tesla they are more differentiated as their separation interval is more than doubled. Comparison of simulated undecoupled spectra at 9.4 Tesla and decoupled spectra at 4 Tesla yielded lower CRB values at 9.4 Tesla, particularly for glutamate and glutamine C2 (data not shown). This suggests that the increased chemical-shift dispersion at 9.4 Tesla can be used to increase the precision on quantitation of ^{13}C-metabolites concentrations even if ^{1}H decoupling is not used.

Indirect Detection

Although this article has focused on ^{13}C NMR spectroscopy without ^{1}H decoupling, another way of investigating brain metabolism in humans at very high fields is by use of indirect ^{13}C detection (^{1}H detection with ^{13}C decoupling). However, using either adiabatic or WALTZ technique to decouple the whole ^{13}C chemical spectrum range in human brain is most likely to be very difficult without exceeding the safety guidelines, as recently demonstrated by de Graaf (28).

Another method is to observe ^{1}H signal without ^{13}C decoupling, as demonstrated by Boumezbeur et al. (12). They were able to follow the ^{13}C time courses of glutamate C3 and C4 in the monkey brain when administrating [U-$^{13}C_6$] glucose. However, in their LCModel analysis, no account of long-range J_{CH} couplings was considered, which consequently might have an effect on the overall time courses observed. The multiplet patterns will change with time when using either undecoupled ^{13}C or undecoupled ^{1}H NMR spectroscopy. However, in the latter case, the observed patterns are unresolved due to small coupling constants resulting from long-range J_{CH} couplings compared to undecoupled ^{13}C NMR where the homonuclear couplings are distinguishable. This in turn might affect the lineshape analysis. It is possible for LCModel to handle this well by considering the sum of the basis sets for every possible isotopomer, but this remains to be shown. Finally, a drawback of indirect detection compared to direct detection is that it was only possible to measure glutamate C3 and C4 time courses. Nevertheless, having more information on the time courses of the different carbon positions of the amino acids and neurotransmitter is helpful for the kinetic modeling of the brain metabolism since fewer assumptions (9) are required to derive metabolic rates like the TCA cycle (major route for glucose metabolism (27,32)) and the glutamate-glutamine cycling (suggested pathway for neuronal activity (33)).

CONCLUSION

This study has shown the feasibility of acquiring and accurately quantifying undecoupled ^{13}C NMR spectra from rat brain at 9.4 Tesla, whereby the time courses of glutamate, glutamine, and aspartate resonances agree very well with those derived from decoupled spectra. Although the SD of these data were slightly higher, ^{13}C NMR without ^{1}H decoupling can greatly simplify the experimental setup by alleviating constraints on electrical isolation of ^{13}C and ^{1}H RF channels and on power deposition imposed by decoupling. In conclusion, this methodology opens the prospect to use ^{13}C NMR spectroscopy to study human brain metabolism at very high magnetic field, therefore enabling further understanding of the function of the normal and disease brain states.

REFERENCES

1. Gruetter R, Adriany G, Choi I-Y, Henry P-G, Lei H, Öz G. Localized in vivo ^{13}C NMR spectroscopy of the brain. NMR Biomed. 2003;16:313–338.
2. de Graaf RA, Mason GF, Patel AB, Behar KL, Rothman DL In vivo ^{1}H-[^{13}C]-NMR spectroscopy of cerebral metabolism. NMR Biomed. 2003;16:339–357.
3. Garcia-Espinosa MA, Rodrigues TB, Sierra A, Benito M, Fonseca C, Gray HL, Bartnik BL, Garcia-Martin ML, Ballesteros P, Cerdan S. Cerebral glucose metabolism and the glutamine cycle as detected by in vivo and in vitro ^{13}C NMR spectroscopy. Neurochem Int. 2004;45:297–303.

4. Criteria for significant risk investigations of magnetic resonance diagnostic devices—guidance for industry and FDA staff. FDA, Center for Devices and Radiological Health, 2003.
5. Medical electrical equipment: particular requirements for the safety of magnetic resonance equipment for medical diagnosis. IEC 2002;601–2–23.
6. Hoult DI, Phil D. Sensitivity and power deposition in a high-field imaging experiment. J Magn Reson Imaging 2000;12:46–67.
7. Collins CM, Liu W, Wang J, Gruetter R, Vaughan JT, Uğurbil K, Smith MB. Temperature and SAR calculations for a human head within volume and surface coils at 64 and 300 MHz. J Magn Reson Imaging 2004;19:650–656.
8. Schwarz AJ, Rijpkema M, Collins DJ, Payne GS, Prock T, Woodward AC, Heerschap A, Leach MO. SAR and tissue heating with a clinical ^{31}P MRS protocol using surface coils, adiabatic pulses, and proton-decoupling. Magn Reson Med 2000;44:692–700.
9. Gruetter R, Seaquist ER, Kim S, Uğurbil K. Localized in vivo ^{13}C-NMR of glutamate metabolism in the human brain: initial results at 4 Tesla. Dev Neurosci 1998;20:380–388.
10. Mason GF, Petersen KF, de Graaf RA, Kanamatsu T, Otsuki T, Rothman DL. A comparison of ^{13}C NMR measurements of the rates of glutamine synthesis and the tricarboxylic acid cycle during oral and intravenous administration of [1-^{13}C] glucose. Brain Res Prot 2003;10:181–190.
11. Gruetter R, Adriany G, Andersen P, Uğurbil K. Feasibility of ^{13}C NMR spectroscopy of the human brain at 7 Tesla using adiabatic ^{1}H decoupling. Proc Intl Soc Mag Reson Med 2001;9:627.
12. Boumezbeur F, Besret L, Valette J, Vaufrey F, Henry P-G, Slavov V, Giacomini E, Hantraye P, Bloch G Lebon V. NMR measurement of brain oxidative metabolism in monkeys using ^{13}C-labeled glucose without a ^{13}C radiofrequency channel. Magn Reson Med 2004;52:33–40.
13. Morris PG, McIntyre DJO, Coxon R, Bachelard HS, Moriarty KT, Green-Haff PL, Macdonald IA. Nuclear magnetic resonance spectroscopy as a tool to study carbohydrate metabolism. Proc. Nutrition Society 1994; 53:335–343.
14. Provencher SW. Estimation of metabolite concentrations from localized in vivo proton NMR spectra. Magn Reson Med 1993;30:672–679.
15. Govindaraju V, Young K, Maudsley AA. Proton NMR chemical shifts and coupling constants for brain metabolites. NMR Biomed 2000;13: 129–153.
16. Kanamori K, Ross BD. In vivo detection of ^{15}N-coupled protons in rat brain by ISIS localization and multiple-quantum editing. J Magn Reson 1999;139:240–249.
17. Henry P-G, Tkáč I, Gruetter R. ^{1}H-localized broadband ^{13}C NMR spectroscopy of the rat brain in vivo at 9.4 T. Magn Reson Med 2003;50: 684–692.
18. Henry P-G, Öz G, Provencher S, Gruetter R. Toward dynamic isotopomer analysis in the rat brain in vivo: automatic quantitation of ^{13}C NMR spectra using LCModel. NMR Biomed 2003;16:400–412.
19. Gruetter R, Tkáč I. Field mapping without reference scan using asymmetric echo-planar techniques. Magn Reson Med 2000;43:319–323.
20. Jeffrey FM, Storey CJ, Sherry AD, Malloy CR. ^{13}C isotopomer model for estimation of anaplerotic substrate oxidation via acetyl-CoA. Am J Physiol 1996;271:E788–E799.
21. Adriany G, Gruetter R. A half-volume coil for efficient proton decoupling in humans at 4 Tesla. J Magn Reson 1997;125:178–184.
22. Bottomley PA, Hardy CJ, Roemer PB. Phosphate metabolite imaging and concentration measurements in human heart by nuclear magnetic resonance. Magn Reson Med 1990;14:425–434.
23. Merkle H, Wei H, Garwood M, Uğurbil K. B_1 Insensitive heteronuclear adiabatic polarization transfer for signal enhancement. J Magn Reson 1992;99:480–494.
24. Klomp DW, Kentgens AP, Heerschap A. Loss-less blocking circuits to combine local quadrature ^{13}C coils with quadrature ^{1}H decoupling coils for human head at 3T. Proc Intl Soc Mag Reson Med 2003;11:2376.
25. Ross B, Lin A, Harris K, Bhattacharya P, Schweinsburg B. Clinical experience with ^{13}C MRS in vivo. NMR Biomed 2003;16:358–369.
26. Gruetter R, Novotny EJ, Boulware SD, Rothman DL, Mason GF, Shulman GI, Shulman RG, Tamborlane WV. Direct Measurement of brain glucose concentrations in humans by ^{13}C NMR spectroscopy. Proc Natl Acad Sci USA 1992;89:1109–1112.
27. Gruetter R, Novotny EJ, Boulware SD, Mason GF, Rothman DL, Shulman GI, Prichard W, Shulman RG. Localized ^{13}C NMR spectroscopy in the human brain of amino acid labeling from D-[1-^{13}C] glucose. J Neurochem 1994;63:1377–1385.
28. de Graaf RA. Theoretical and experimental evaluation of broadband decoupling techniques for in vivo nuclear magnetic resonance spectroscopy. Magn Reson Med 2005;53:1297–1306.
29. Vaughan JT, Garwood M, Collins CM, Liu W, DelaBarre L, Adriany G, Andersen P, Merkle H, Goebel R, Smith MB. Uğurbil K. 7T vs. 4T: RF power, homogeneity, and signal-to-noise comparison in head images. Magn Reson Med 2001;46:24–30.
30. Collins CM, Li S, Smith MB. SAR and B_1 field distributions in a heterogeneous human head model within a birdcage coil. Magn Reson Med 1998;40:847–856.
31. Uğurbil K, Adriany G, Andersen P, Chen W, Garwood M, Gruetter R, Henry P-G, Kim S-G, Lieu H, Tkáč I, Vaughan T, Van De Moortele PF, Yacoub E, Zhu X. Ultrahigh field magnetic resonance imaging and spectroscopy. Magn Reson Imaging 2003;21:1263–1281.
32. Beckmann N, Turkalj I, Seelig J, Keller U. ^{13}C NMR for the assessment of human brain glucose metabolism in vivo. Biochemistry 1991;30: 6362–6366.
33. Sibson NR, Dhankhar A, Mason GF, Behar KL, Rothman DL, Shulman RG. In vivo ^{13}C NMR measurements of cerebral glutamine synthesis as evidence for glutamate-glutamine cycling. Proc Natl Acad Sci USA, 1997;94:2699–2704.